HHS Public Access

Author manuscript

Comput Methods Programs Biomed Update. Author manuscript; available in PMC 2023 July 20.

Published in final edited form as:

Comput Methods Programs Biomed Update. 2023 ; 3: . doi:10.1016/j.cmpbup.2023.100107.

Rianú: Multi-tissue tracking software for increased throughput of engineered cardiac tissue screening

Jack F. Murphy,

Kevin D. Costa,

Irene C. Turnbull*

Icahn School of Medicine at Mount Sinai, One Gustave L. Levy Place, Box 1014, New York City, 10029, NY, USA

Abstract

Background: The field of tissue engineering has provided valuable three-dimensional species-specific models of the human myocardium in the form of human Engineered Cardiac Tissues (hECTs) and similar constructs. However, hECT systems are often bottlenecked by a lack of openly available software that can collect data from multiple tissues at a time, even in multi-tissue bioreactors, which limits throughput in phenotypic and therapeutic screening applications.

Methods: We developed Rianú, an open-source web application capable of simultaneously tracking multiple hECTs on flexible end-posts. This software is operating system agnostic and deployable on a remote server, accessible via a web browser with no local hardware or software requirements. The software incorporates object-tracking capabilities for multiple objects simultaneously, an algorithm for twitch tracing analysis and contractile force calculation, and a data compilation system for comparative analysis within and amongst groups. Validation tests were performed using in-silico and in-vitro experiments for comparison with established methods and interventions.

Results: Rianú was able to detect the displacement of the flexible end-posts with a sub-pixel sensitivity of 0.555 px/post (minimum increment in post displacement) and a lower limit of 1.665 px/post (minimum post displacement). Compared to our established reference for contractility assessment, Rianú had a high correlation for all parameters analyzed (ranging from $R^2 = 0.7514$ to $R^2 = 0.9695$), demonstrating its high accuracy and reliability.

*Corresponding author. irene.turnbull@mssm.edu (I.C. Turnbull).

Declaration of competing interest

The authors declare the following financial interests/personal relationships which may be considered as potential competing interests: K.D.C. holds equity in NovoHeart Holdings. NovoHeart did not contribute to the funding, planning, or execution of this study; however, the study outcomes could potentially have a financial impact on NovoHeart. The other authors declare that they have no competing interests.

CRediT authorship contribution statement

Jack F. Murphy: Conceptualization, Methodology, Software, Investigation, Data curation, Writing – original draft. **Kevin D. Costa:** Writing – review & editing, Supervision, Funding acquisition. **Irene C. Turnbull:** Conceptualization, Investigation, Writing – review & editing, Supervision, Funding acquisition.

Appendix A. Supplementary data

Supplementary material related to this article can be found online at https://doi.org/10.1016/j.cmpbup.2023.100107.

Conclusions: Rianú provides simultaneous tracking of multiple hECTs, expediting the recording and analysis processes, and simplifies time-based intervention studies. It also allows data collection from different formats and has scale-up capabilities proportional to the number of tissues per field of view. These capabilities will enhance throughput of hECTs and similar assays for in-vitro analysis in disease modeling and drug screening applications.

Keywords

Tissue engineering; Object tracking; Cardiac muscle function; Human engineered cardiac tissues; Contractility analysis; Drug screening

1. Introduction

Human engineered cardiac tissues (hECTs) are valuable constructs that provide 3-D species-specific models of the human myocardium for in-vitro assessments. hECTs have widespread appeal due to their unique ability to recapitulate functional properties of the myocardium and have shown promise as a preclinical model for drug screening [1,2]. Our group and others have developed independent hECT systems for quantifying tissue function [3–7]. One shortcoming in the field is that the quantitative analysis software for each system is often custom tailored for a particular bioreactor design. This bioreactor dependency of the analysis tools means that every group that wants to develop a novel bioreactor needs to develop tracking software concurrently, deterring development and hindering advances in cardiac tissue engineering. Additionally, while bioreactors have progressed to allow for the culture of up to six hECTs in a shared media environment [3], there lacks a suitable openly available software to collect data from all tissues in parallel. This results in discontinuous data collection, with the need to reposition the bioreactor for video recording of each hECT, and also requires repeated electrical stimulation that would be avoided if multiple tissues were tracked simultaneously. This restriction renders multi-tissue systems ineffectual in studies where an effect occurs soon after the intervention [8], or for dose-dependent experiments where incremental dosages are applied within 3 min of each other [2,9], or even for 10 min step recording, the current system would still pose a challenge [10]. Even though multiple tissues can receive a treatment at the same time point, to our knowledge there is no open access software that would permit data to be collected from them simultaneously. Software capable of tracking multiple hECTs in parallel can reduce recording time, increase throughput, and allow experimental studies where multiple tissues in a bioreactor are exposed to an intervention and it would be beneficial to acquire responses simultaneously.

Two main approaches to evaluating hECT function are optical recording and tensile testing. The tensile testing technique is very intrusive, requiring the removal of the hECTs from their bioreactor and attachment to force sensors and length controllers [5,7]. This requires specialized instrumentation, damages the ends of tissues, and prevents capturing contractile function data on subsequent days. Optical recording platforms solve some of these issues by not requiring tissue handling and allowing longitudinal studies, but a comprehensive, validated, open-access software package to quantify recorded tissue contractility is lacking. Existing optical recording analysis software suffers from limitations such as either being

unable to obtain contractile forces, requiring commercial recording hardware, or being limited to recording one hECT at a time [3,6,11,12].

In this study, we present a new open-source web application capable of tracking multiple hECTs simultaneously; this shortens recording times, reduces bioreactor manipulation and avoids tissue exposure to unnecessary repeated electrical stimulation. This software offers the latest advance in our efforts to track contractility features in hECTs. Furthermore, its versatility allows for data collection from tissues of various different formats. These characteristics address a major bottleneck in the functional assessment of hECTs caused by the limitations of currently available open-access software.

2. Material and methods

2.1. Rianú algorithm

Rianú is an open-source web application capable of obtaining valuable cardiac muscle function parameters from videos of hECT contractions. Rianú is primarily written in Python [13], with simple operating system agnostic deployment made possible using Docker containers [14]. The software was designed to be deployed on a remote server and interacted with via a web browser, but it can be run locally if the user prefers, and provides many advantages over our established software (Supplementary Table S1).

2.1.1. Post tracking—Posts are tracked through each video frame using an OpenCV [15] implementation of a Discriminative Correlation Filter with Channel and Spatial Reliability (DCF-CSR) tracker [16]. The user supplies starting post locations through drawing boxes on the first frame. One DCF-CSR tracker is spawned per post and follows that post through subsequent frames. The difference of the centroids for each pair of posts is taken and used to obtain the total post deflection of each tissue. The associated time for each deflection is obtained from the frame properties using OpenCV's CAP_PROP_POS_MSEC function.

2.1.2. Force calculations—Force is derived from individual post deflections using the beambending equation (Eq. (1)) [17], where δ is displacement, a is the distance between the tissue and the base of the post (tissue height), L is the post height, E is Young's modulus of the post, R is post radius and subscripts denote left post (L), right post (R), or total (T).

$$F_L = \frac{3\pi E R_L^4}{2a_L^2(3L_L - a_L)} * \delta_L \quad (1)$$

Eq. (1) applies to each post independently meaning that δ_L and δ_R must be calculated from δ_T, when $\delta_T = \delta_R + \delta_L$. Since the tissue is taut between two posts the force applied to each post must equal. Setting $F_L = F_R$ and simplifying allows for Eq. (2) to be applied to the total displacement to obtain individual post displacements.

$$\delta_L = \frac{\delta_T}{1 + \frac{\delta_R}{\delta_L}} \text{ where } \frac{\delta_R}{\delta_L} = \frac{a_R^2(3L_R - a_R)}{a_L^2(3L_L - a_L)} \quad (2)$$

2.1.3. Data processing—The raw force data is smoothed using a Savitzky-Golay filter (sav-gol) as supplied by the SciPy signal processing python package to allow for easier visualization and analysis [18,19]. A sav-gol filter uses linear least-squares regression to smooth data. Two variables control how this smoothing occurs, the polynomial degree to which the data is fitted and the window size, which is the number of coefficients (Supplementary Table S2). The window size must be a positive odd integer and larger than the polynomial. The larger the difference between the polynomial and window size, the smoother the signal will be, which means that to reduce signal distortion these values should be kept as close as possible while still smoothing the data enough for analysis. The sav-gol filter fits local polynomials to each point as part of the smoothing process, those polynomial slopes are taken as the dF/dt function, which is used to find the +dF/dt and −dF/dt. Further data processing can be undertaken in select situations. If the tracked objects move away from each other during a contraction, the data can be inverted prior to peak finding. Additionally, if there is an artificial trend, the linear trend of the data can be removed. This should only be done in select situations as it will unfairly alter the systolic and diastolic forces. It is important that data with sufficient temporal resolution is supplied to the smoothing algorithm so that it does not omit peak values, this becomes more important when higher frequencies are investigated. For all videos analyzed in this paper the number of frames per second (FPS) was ≥30.

2.1.4. Peak detection—Peaks are detected after smoothing using the find_peaks function supplied in the SciPy signal processing package. Two parameters are used in finding peaks, the prominence and minimum distance. The prominence is a relative value between zero and one that measures how much the peak protrudes from values around it, while the minimum distance is how large of an interval is required between peaks (an interval length is measured by the number of data points). These two parameters combined allow for user correction if the algorithm incorrectly identifies noise as a contraction peak.

2.1.5. Twitch characterization—From each peak moving backward and forward chronologically, the first-order derivative crossing zero defines the beginning and end of each contraction, respectively. The force at the beginning and end of the twitch is averaged to get a baseline for the twitch. This baseline force and the peak force (maximum contraction force) are used to calculate the force values at 10% and 50% contracted, and 50% and 90% relaxed. If no data point falls exactly at this force, a linear approximation is used between the closest point on either side. These points are used to calculate parameters of cardiac muscle function as summarized in Table 1. For values described in Table 1 all parameters except BF and BF CoV are calculated once per contraction, the values from multiple contractions are used to obtain a mean ± standard deviation. BF is calculated for each interbeat interval and used to obtain mean ± standard deviation. BF CoV is then calculated by taking the BF and corresponding standard deviation. We recommend

analyzing at least ten contractions for a reliable mean, this system can also be applied to fewer contractions at the users' discretion. One parameter can be used to correct in case of misidentification of the start or end of a twitch, the buffer. The buffer is how many data points away from the peak the algorithm should wait before looking for the derivative change.

2.1.6. Data archival—Calculated twitch characteristics are available for download as an excel file for each set of tissues analyzed. Additionally, a zip file containing all videos, excel files, and related database metadata can be downloaded for long-term archival when an experiment has concluded. That zip file can be re-uploaded later, and the database will automatically be populated with the previously used bioreactor and calibration data.

2.2. In-silico hECT model

For in-silico simulations we developed a custom MATLAB script, available at DOI: 10.17605/OSF.IO/YWCHZ, to simulate video recordings of sine-based post displacements (30 FPS, 1920×1080px, 111 px/mm, .mp4). Each video contained 6 pairs of black dots that moved towards each other at the assigned frequency and displacement. The assigned displacements included 1.665, 2.22, 3.33, 4.44, 5.55, 11.1, and 22.2 px/post. Each of these displacements were generated at frequencies of 0.75, 1.00, and 1.25 Hz. Analysis of this in-silico model assumed post heights of 3 mm, distance between posts as 6 mm, Young's modulus as 1.33 MPa, and post radii as 0.277 mm. Sav-gol smoothing parameters were kept constant with a polynomial of 3 and a window size of 19.

2.3. In-vitro hECT model

Human engineered cardiac tissues were fabricated as previously described [3]. Human induced pluripotent stem cells (hiPSCs) from a healthy cell line (SKiPS 31.3, [20]) were differentiated into cardiomyocytes. After day 25 of differentiation the hiPSC-derived cardiomyocytes were collected and resuspended in a Collagen and Matrigel mix (Bovine Collagen type I and Matrigel). This mix was layered onto a custom baseplate fitted with a polysulfone frame holding PDMS molds. The multi-tissue bioreactor holds up to six hECTs, each hECT is held between two flexible PDMS cantilever posts, and they share the same media bath in culture [3]. Functional analysis of the hECTs with our established reference and Rianú were performed after day 10 of hECT fabrication.

2.4. Established reference software

To evaluate the contractile function of the hECT, tissues were viewed one at a time using a dissecting microscope equipped with a Pixelink PL-B741 camera connected to a Olympus SZ61 dissecting microscope. Previously established software was then used to track (LabVIEW, National Instruments) and analyze (MATLAB, MathWorks) hECT function, serving as the control for validating this software for in-vitro experiments [21]. A custom LabVIEW script performed real-time tracking on two posts, saving centroid locations to a .dat file. Post and tissue heights needed in Eq. (1) were then manually entered into a summary CSV file. That summary CSV file and the .dat files was supplied to a custom MATLAB script that performed data smoothing, peak finding, and twitch parameter

calculations [3]. For all analysis of in-vitro hECTs sav-gol polynomial was 4 with a window size of 11 in both systems.

2.5. In-vitro pharmacologic applications

The hECTs were placed in a laminar flow hood, on a heating stage table, and visualized with a dissecting microscope equipped with a camera connected to a computer as described above. Video recordings, including three hECT per frame, were obtained under spontaneous conditions. The recordings started (pre-treatment), then isoproterenol (Isoproterenol hydrochloride; Sigma-Aldrich, Catalog #: I5267) was dispensed into the media for a final concentration of 300 nM. The hECTs were monitored and recordings were also obtained ten minutes after isoproterenol administration (post-treatment). The pre-treatment and ten minute post-treatment recordings were uploaded to Rianú for analysis.

2.6. Non-cantilever applications

To test Rianú on systems that are not cantilever dependent, two hECTs were fabricated using the same method described in Section 2.3 with minor modifications described hereafter. As one example of a non-cantilever dependent system, one hECT was unhooked from both posts after 7 days in culture, one day later functional analysis was performed, this was used to track the contraction of a free-floating tissue. As another example of a non-cantilever dependent system, we aimed to emulate a quasi-circular shaped hECT. For that purpose we accelerated the compaction of the hECT through supplementation with human ventricular cardiac fibroblasts (Lonza, Catalog #: CC-2904) at the time of fabrication [22]. After seven days in culture the hECT was unhooked from one post and by day ten the tissue had compacted and curled up around the top of a single post, this was used to track contractions of a circular shaped hECT.

2.7. Statistical analysis

Data were analyzed and graphed in Prism (GraphPad) and R 4.0.4 [23]. Data are presented as mean ± standard deviation. Differences between two experimental groups containing the same tissues were analyzed by paired two-tailed Student's t-test. Differences between more than two independent experimental groups were analyzed by oneway ANOVA, significant results ($P < 0.05$) were followed by Bonferroni post hoc test. Linear least-squares regression was performed to compare outputs from Rianú to the assigned inputs of the in-silico model; and also to compare outputs from Rianú and our established reference. Significant differences defined by $P < 0.05$ (*), $P < 0.01$ (**), $P < 0.001$ (***), and $P < 0.0001$ (****).

3. Results

3.1. Implementation

To increase throughput of experiments involving engineered cardiac tissue constructs, we developed Rianú. Rianú is an open-source web application capable of tracking and analyzing multiple hECTs simultaneously. This software was designed to be operating system agnostic and deployed on a remote server, accessible via a web browser with no local hardware or software requirements. Each Rianú instance has a database that stores bioreactor, hECT, and calibration information needed for cardiac contractility assessment. Instances can be

personal and password protected or shared between multiple users if they use the same bioreactors.

We and others have used a dual cantilever bioreactor setup to quantify hECT contractility [3,6,7,24,25]. In this setup, a tissue is fabricated suspended between two flexible polydimethylsiloxane (PDMS) posts, when the tissue contracts it pulls on both cantilever posts causing them to deflect inwardly. The post deflections can be converted into a measurement of force (described in detail in Section 2.1.2).

The workflow for using Rianú to analyze cardiac tissue function of this setup breaks down into four parts (Fig. 1). Firstly, a video of the post deflections caused by tissue contractions needs to be obtained and uploaded to Rianú (Fig. 1.A, Supplementary Video S1). As part of this upload process, metadata needed for analysis such as post and tissue heights are either inputted or selected from the database. Secondly, once a video has been uploaded, it can be tracked; the user selects the video and draws starting post locations on the first frame (Fig. 1.B). The tracking algorithm takes those starting positions and follows each post through subsequent frames, calculating the centroid of each post and saving the raw post deflection data. Thirdly, after tissues have been tracked, they can be analyzed (Fig. 1.C). The user selects the tissues of interest; the raw deflection data is then converted into a force as described in Eq. (1). Rianú then smooths the raw force data and finds the peaks (see Section 2.1 for details). The peaks are used to calculate twitch parameters, and calculated parameters are outputted to a CSV file. Finally, after an experiment is finished, Rianú allows archival of data through a zip download (Fig. 1.D). The user selects the experiment they want to archive, which downloads a zip file containing all videos, twitch parameters, post locations, and bioreactor metadata related to that experiment. The experiment can then be deleted from the server and stored offline; if reanalysis is ever needed, that zip file can be uploaded, which will upload the archived videos and populate the database with all required metadata.

3.2. In silico characterization of sensitivity, reliability, and repeatability

The sensitivity, reliability, and repeatability of Rianú's post-deflection tracking capabilities were characterized using a custom in-silico hECT model with assigned post displacement amplitudes and frequencies ranging from 1.665 px/post to 22.2 px/post and 0.75 to 1.25 Hz (with 0.25 Hz increments), respectively. Each contraction frequency was analyzed at all post displacement amplitudes, and no significant differences in measured beating frequency (BF) were observed across displacement amplitude groups for each assigned frequency ($P = 0.941$ for 0.75 Hz, $P = 0.991$ for 1 Hz, $P = 0.995$ for 1.25 Hz; Fig. 2.A and Supplementary Table S3). Linear least-squares regression analysis confirmed the expectation that the measured BF is linearly correlated with the assigned BF $\left(R^2 = 0.9998\right)$ (Fig. 2.B). The developed force (DF) was measured for all assigned post displacement amplitudes; the resulting DF was significantly different between all post displacement amplitude groups, with higher DF at each increasing post displacement amplitude (ANOVA $P < 0.0001$; Bonferroni post hoc $P < 0.0001$ for each groupwise comparison; Fig. 2.C). This demonstrates that Rianú was able to reliably detect post displacement differences with a subpixel sensitivity of 0.555 px/post (minimum increment between post displacements) and a lower limit of 1.665 px/post (minimum post displacement). The repeatability of this software was tested

through the repeated tracking and analysis of a video with assigned deflections of 5.55 px/post (Supplementary Video S2), it was repeated ten times using the same data smoothing parameters each time and the results were consistent across all iterations with no significant differences between trials for BF ($P = 0.888$) or DF ($P = 0.493$).

3.3. Correlation to established reference

We then sought to evaluate Rianú's performance compared to our validated system (established reference) currently used to record and analyze post deflections of individual hECTs [3]. A screen recording was captured while the contractions of the hECTs were tracked in real-time using the existing established reference software. The screen recording was uploaded to Rianú, allowing for post hoc tracking and analysis of the same hECT twitches. After tracking and analysis, the outputs from both systems showed a high correlation for all twitch characteristics investigated, including force- and time-domain parameters. Measurements under both electrical field stimulation (Fig. 3.A) and spontaneous beating (Fig. 3.B) conditions were analyzed. The high correlation for DF (Fig. 3.A.1), systolic force (Fig. 3.A.2) and diastolic force (Fig. 3.A.3) as well as the time to peak force (T2PK, Fig. 3.A.4) display Rianú's ability to detect inotropic changes in hECTs. The time-domain parameter correlations including time to 50% relaxation (R50, Fig. 3.A.5), time to 90% relaxation (R90, Fig. 3.A.6), and spontaneous BF (Fig. 3.B.1), show Rianú's ability to detect lusitropic and chronotropic changes. The maximum rates of contraction (+dF/dt, Fig. 3.A.7) and relaxation (−dF/dt, Fig. 3.A.8) can be affected by both inotropic and chronotropic changes. The beating frequency coefficient of variation (BF CoV, Fig. 3.B.2) correlation shows Rianú's ability to detect beating frequency irregularity, which can be used to detect a proarrhythmic phenotype [1]. The force-frequency relationship is another indicator of cardiac contractility, we evaluated how this measurement compared between Rianú and the established reference and observed mirrored trends in both (Fig. 3.C).

3.4. In-vitro pharmacological applications

Rianú successfully detected chronotopic changes in hECT contractions in response to isoproterenol [300 nM] under spontaneous conditions. Videos recording spontaneous contractions of the hECTs were obtained before, during, and for ten minutes after isoproterenol administration (Supplementary Video S3). For comparison of the BF changes in response to isoproterenol, two thirty-second video segments were analyzed pre-treatment and ten minutes post-treatment. The hECTs showed a 2.51 ± 0.26 fold increase in spontaneous BF ($P < 0.0001$; Fig. 4.A), with a significant decrease in BF CoV ($P = 0.009$; Fig. 4.B). DF did not change significantly ($P = 0.591$). T2PK, time to 50% relaxation (R50) and time to 90% relaxation (R90) decreased after isoproterenol, but the difference was not significant (Figure S1). Representative twitch tracings of force and dF/dt are shown in Fig. 4.C and D. Of note, the change in BF was rapid; an increase in BF was identified within the first 60 s after isoproterenol administration (2.66 ± 0.86 fold increase compared to pre-treatment).

3.5. Application to other bioengineered cardiac platforms

Not all 3-D tissue culture models of human myocardium include cantilever posts [26–29]. In order to demonstrate that Rianú is not limited to acquiring data from only cantilever-based bioreactors, both a free-floating tissue (Supplementary Video S4) and a tissue only anchored on one post (Supplementary Video S5) were recorded under electrical field stimulation. In both experimental conditions, the beating frequency matched the applied 1.00 Hz electrical stimulation frequency; with measured BFs of 0.99 ± 0.036 (3.6% BF CoV) Hz and 1.00 ± 0.047 Hz (4.7% BF CoV) for the free-floating and single post anchored tissues, respectively (Fig. 5). Video S6 and Figure S2 shows a straightforward application of Rianú to an alternative arrangement of 6 cardiac tissues using the multiwell assay from EHT technologies; the post characteristics included in the analysis to calculate the absolute force are described in [6,17,30]. These results serve as proof-of-concept for Rianú's capability to be applied to varied hECT experimental setups. We also tested Rianú's applicability to other bioengineered cardiac platforms. Video S7 and Figure S3 demonstrate monitoring single cardiomyocyte contractility by tracking fluorescent beads displacement in a traction force microscopy assay, from Sala et al. [12]. Video S8 and Figure S4 shows monitoring the contractions of two free floating engineered heart muscle (EHM) tissue rings by tracking the edges of the tissues, showing differences in spontaneous beating rate for the different EHM compositions, from Tiburcy et al. [31]. Video S9 and Figure S5 demonstrate five displacement tracings obtained from tracking ten flexible holders around the periphery of an EHM patch, from Tiburcy et al. [31]. Finally, we used Rianú to examine the contraction of a monolayer culture of hiPSC-CMs, segmented into 36 regions, we applied 18 individual tracking features, demonstrating regional differences in myocyte beating pattern (Video S10, Figure S6). These examples demonstrate the versatility of the Rianú software, including the ability to simultaneously track a large number of features as required for applications such as high throughput screening.

4. Discussion

Our previous work shows how multiple tissues cultured in a shared media environment serve as a system to explore cell–cell interactions and dissect paracrine effects [32,33]. This bioreactor potentially allows for synchronous recording of multiple tissue responses to external stimuli; however, this multi-tissue capability has not been realized to date due to a lack of available software implementing the capturing of video data from more than one tissue at a time. Previously available software has been too specific, only working for particular bioreactor configurations, requiring commercial hardware [6], or limiting the number of tissues that can be analyzed [3]. Alternatively, open-source software exists that is capable of capturing data from a variety of culture conditions, but force is reported in arbitrary units, and even the latest version appears to capture data from one tissue at a time [12].

Rianú's use of a general-purpose tracker makes it uniquely versatile. Rianú reliably detected hECT contractions; in cases where the experimental setup allows (i.e. dual cantilever suspended hECTs), those contractions were translated into forces; and in experimental setups that have no way to translate contraction displacements to forces (i.e. free-floating

hECTs), Rianú was applied to report time-domain parameters, as demonstrated by our proof-of-concept test (Fig. 5). The open-source nature of this software further builds on this versatility, as the same tracking software can be re-purposed for non-cantilever bioreactor setups, or for systems with alternative equations to translate displacement into force values. Rianú accepts video recordings, which allows for re-analysis of the same video multiple times, or by multiple investigators, if comparisons at a later time point are desired (Supplementary Table S1).

In this study, we limited our simulations to six in-silico tissues because that is currently the highest quantity of hECT that our experimental bioreactor system can culture in a shared media environment [3]. However, this is not a software limitation, and Rianú can track a higher number of objects, limited only by the experimental setup's ability to capture displacements greater than 1.665 pixels per object of interest. Rianú's ability to increase throughput is determined as a factor of the number of trackable objects in the recording; applied to our multi-tissue bioreactor that holds 6 hECTs, this translates to a 6-fold increase in throughput. Tracking this in silico model (Video S2) with 6 tissues took under 1 min (10 s, 1920 × 1080, 25 fps). As an example of further parallel analysis, we used a video of a engineered heart muscle patch configuration with multiple flexible holders, described and shown in Tiburcy et al. (Video S9 [15 s, 306 × 218, 50 fps]) [31], we tracked the motion from a combination of 24 pairs of objects (48 trackers) and completed the analysis in under 3 min.

Rianú is an entirely post hoc implementation of hECT analysis. It does not help with hECT fabrication or recording. This, however, leaves the user with flexibility on how they want to generate and record hECTs; they do not need to limit themselves to any particular setup. In the experimental setup design, consideration needs to be taken to use a camera of sufficient frame rate, zoom, and resolution to obtain displacements of higher than 1.665 pixels per object of interest as Rianú struggled with displacements lower than this. This practical lower limit in detection displacement is a result of the CSRT localization process attempting to find the object of interest within the region of interest, which introduces minor jitter of the tracker boundaries. In silico simulations found object displacements lower than 1.665 px were obfuscated by this intrinsic jitter, while larger displacements were able to overcome this baseline jitter and get a readable signal with a 0.555 px sensitivity. Deep learning trackers could be implemented to address these sensitivity limitations as long as the object of interest is consistent across recordings.

For applications where the same objects are tracked in every video, a deep learning based Generic Object Tracking Using Regression Networks tracker (GOTURN) could be trained to increase object tracking accuracy and speed [34]. In addition, object detection could be automated using contour detection or deep learning [35,36], eliminating the need to manually draw each object's starting position; indeed, future versions of Rianú could use AI-based feature tracking rather than manual ROI selection. Teles et al. have shown the use of machine learning to identify healthy or diseased cardiomyocytes based on twitch tracing data [37]. Additionally, Lee et al. have used machine learning for comprehensive analysis of contractile behavior in drug screening studies [2]. Rianú's use of Python, a popular language for machine learning, and its deployment on a server makes it well suited for fully

integrating these machine learning approaches to automate tissue characterization, with the advantage of not requiring additional steps in the user workflow. Combining deep learning trackers with machine learning characterization techniques would expedite Rianú at every step of the process, including post detection, post tracking, and functional characterization. The implementation of these techniques was outside of the scope of our study, but we envision that Rianú could be used to train these machines. In consideration of the recent FDA Modernization Act 2.0 [38], there is growing interest in using in vitro cardiac assays for drug development, and we anticipate that analysis techniques such as Rianú will have an important role for future regulatory requirements.

In conclusion, herein we present a fully open-source software designed to be deployable on a remote server and accessed via any web browser. This software reliably detects hECT contractions and translates them into twitch tracings which are used to obtain measurements for DF, BF, and other associated cardiac muscle function parameters. The ease of implementation, availability, and versatility of this software will help advance hECT studies. Its multi-tracking capabilities make it practical to evaluate multiple hECTs recorded simultaneously, increasing throughput of hECT screening.

Supplementary Material

Refer to Web version on PubMed Central for supplementary material.

Acknowledgments

We acknowledge Brendan T. Murphy for his valuable contributions to the software development. The engineered heart tissues (EHTs) shown in Video S6 were generously provided by Dr. Nicole Dubois and Dr. Nadeera Wickramasinghe, Icahn School of Medicine at Mount Sinai.

Funding

This work was funded by the National Heart, Lung, and Blood Institute of the National Institutes of Health, USA under Award Number R03HL154286 (ICT), K01HL133424 (ICT) and R01HL132226 (KDC). The content is solely the responsibility of the authors and does not necessarily represent the official views of the National Institutes of Health.

Data availability

Source code for Rianú is stored on gitlab with the canonical URL https://gitlab.com/hECT-Software/rianu and accessible via the open science framework (OSF) with the DOI: 10.17605/OSF.IO/YWCHZ along with raw data reported in this study, the R scripts used to perform statistics and present figures, the in-silico model, full installation instructions, and all supplemental material.

Standard OpenCV CRST object trackers were adopted for use in this software while novel code was developed for the web interface including file upload, bioreactor and experiment management, calibration, region of interest selection, and twitch tracing analysis. Libraries such as SciPy were leveraged to perform operations such as Sav-gol smoothing and peak finding while new code was developed to find the start, end, 10, 50, 90% relaxed and 10, 50, 90% contracted points used for twitch parameter calculation.

References

[1]. Schaaf S, Shibamiya A, Mewe M, Eder A, Stöhr A, Hirt MN, Rau T, Zimmermann W-H, Conradi L, Eschenhagen T, Hansen A, Human engineered heart tissue as a versatile tool in basic research and preclinical toxicology, PLoS One 6 (10) (2011) e26397, 10.1371/journal.pone.0026397. [PubMed: 22028871]

[2]. Lee EK, Tran DD, Keung W, Chan P, Wong G, Chan CW, Costa KD, Li RA, Khine M, Machine learning of human pluripotent stem cell-derived engineered cardiac tissue contractility for automated drug classification, Stem Cell Rep. 9 (5) (2017) 1560–1572, 10.1016/j.stemcr.2017.09.008, Publisher: Cell Press.

[3]. Turnbull IC, Mayourian J, Murphy JF, Stillitano F, Ceholski DK, Costa KD, Cardiac tissue engineering models of inherited and acquired cardiomyopathies, in: Methods in Molecular Biology (Clifton, N.J.), Vol. 1816, Springer New York, 2018, pp. 145–159.

[4]. Nunes SS, Miklas JW, Liu J, Aschar-Sobbi R, Xiao Y, Zhang B, Jiang J, Massé S, Gagliardi M, Hsieh A, Thavandiran N, Laflamme MA, Nanthakumar K, Gross GJ, Backx PH, Keller G, Radisic M, Biowire: a platform for maturation of human pluripotent stem cell-derived cardiomyocytes, Nature Methods 10 (8) (2013) 781–787, 10.1038/nmeth.2524. [PubMed: 23793239]

[5]. Kaiser NJ, Munarin F, Coulombe KLK, Custom engineered tissue culture molds from laser-etched masters, J. Vis. Exp. (135) (2018) 10.3791/57239, Publisher: MyJove Corporation.

[6]. Mannhardt I, Saleem U, Benzin A, Schulze T, Klampe B, Eschenhagen T, Hansen A, Automated contraction analysis of human engineered heart tissue for cardiac drug safety screening, J. Vis. Exp. (122) (2017) 10.3791/55461.

[7]. Ronaldson-Bouchard K, Ma SP, Yeager K, Chen T, Song L, Sirabella D, Morikawa K, Teles D, Yazawa M, Vunjak-Novakovic G, Advanced maturation of human cardiac tissue grown from pluripotent stem cells, Nature 556 (7700) (2018) 239–243, 10.1038/s41586-018-0016-3. [PubMed: 29618819]

[8]. Arai K, Murata D, Takao S, Nakamura A, Itoh M, Kitsuka T, Nakayama K, Drug response analysis for scaffold-free cardiac constructs fabricated using bio3D printer, Sci. Rep. 10 (1) (2020) 1–11, 10.1038/s41598-020-65681-y, Publisher: Nature Publishing Group. [PubMed: 31913322]

[9]. Jonsson MK, Wang QD, Becker B, Impedance-based detection of beating rhythm and proarrhythmic effects of compounds on stem cell-derived cardiomyocytes, Assay Drug Dev. Technol. 9 (6) (2011) 589–599, 10.1089/adt.2011.0396, Publisher: Mary Ann Liebert, Inc.. [PubMed: 22085047]

[10]. Kaneko T, Nomura F, Hamada T, Abe Y, Takamori H, Sakakura T, Takasuna K, Sanbuissho A, Hyllner J, Sartipy P, Yasuda K, On-chip in vitro cell-network pre-clinical cardiac toxicity using spatiotemporal human cardiomyocyte measurement on a chip, Sci. Rep. 4 (1) (2014) 1–8, 10.1038/srep04670, Publisher: Nature Publishing Group.

[11]. Ronaldson-Bouchard K, Yeager K, Teles D, Chen T, Ma S, Song LJ, Morikawa K, Wobma HM, Vasciaveo A, Ruiz EC, Yazawa M, Vunjak-Novakovic G, Engineering of human cardiac muscle electromechanically matured to an adult-like phenotype, Nat. Protoc. 14 (10) (2019) 2781–2817, 10.1038/s41596-019-0189-8, Publisher: Nature Publishing Group. [PubMed: 31492957]

[12]. Sala L, Van Meer BJ, Tertoolen LG, Bakkers J, Bellin M, Davis RP, Denning C, Dieben MA, Eschenhagen T, Giacomelli E, Grandela C, Hansen A, Holman ER, Jongbloed MR, Kamel SM, Koopman CD, Lachaud Q, Mannhardt I, Mol MP, Mosqueira D, Orlova VV, Passier R, Ribeiro MC, Saleem U, Smith GL, Burton FL, Mummery CL, Musclemotion: A versatile open software tool to quantify cardiomyocyte and cardiac muscle contraction in vitro and in vivo, Circ. Res. 122 (3) (2018) e5–e16, 10.1161/CIRCRESAHA.117.312067, Publisher: Lippincott Williams & Wilkins Hagerstown, MD. [PubMed: 29282212]

[13]. Python Software Foundation, Python, 2021, URL https://github.com/python/cpython.

[14]. Merkel D, Docker: Lightweight linux containers for consistent development and deployment, Linux J. 2014 (239) (2014) Publisher: Belltown Media.

[15]. Bradski G, The openCV library, Dr. Dobb's J. Softw. Tools 25 (11) (2000) 120–123, Publisher: Miller Freeman Inc..

[16]. Lukežič A, Vojíř T, Zajc LČ, Matas J, Kristan M, Discriminative correlation filter tracker with channel and spatial reliability, Int. J. Comput. Vis. 126 (7) (2018) 671–688, 10.1007/s11263-017-1061-3.

[17]. Vandenburgh H, Shansky J, Benesch-Lee F, Barbata V, Reid J, Thorrez L, Valentini R, Crawford G, Drug-screening platform based on the contractility of tissue-engineered muscle, Muscle Nerve 37 (4) (2008) 438–447, 10.1002/mus.20931, Publisher: John Wiley & Sons, Ltd. [PubMed: 18236465]

[18]. Savitzky A, Golay MJ, Smoothing and differentiation of data by simplified least squares procedures, Anal. Chem. 36 (8) (1964) 1627–1639, 10.1021/ac60214a047, Publisher: American Chemical Society.

[19]. Virtanen P, Gommers R, Oliphant TE, Haberland M, Reddy T, Cournapeau D, Burovski E, Peterson P, Weckesser W, Bright J, van der Walt SJ, Brett M, Wilson J, Millman KJ, Mayorov N, Nelson ARJ, Jones E, Kern R, Larson E, Carey CJ, Polat İ, Feng Y, Moore EW, VanderPlas J, Laxalde D, Perktold J, Cimrman R, Henriksen I, Quintero EA, Harris CR, Archibald AM, Ribeiro AH, Pedregosa F, van Mulbregt P, Vijaykumar A, Bardelli AP, Rothberg A, Hilboll A, Kloeckner A, Scopatz A, Lee A, Rokem A, Woods CN, Fulton C, Masson C, Häggström C, Fitzgerald C, Nicholson DA, Hagen DR, Pasechnik DV, Olivetti E, Martin E, Wieser E, Silva F, Lenders F, Wilhelm F, Young G, Price GA, Ingold G-L, Allen GE, Lee GR, Audren H, Probst I, Dietrich JP, Silterra J, Webber JT, Slavič J, Nothman J, Buchner J, Kulick J, Schönberger JL, de Miranda Cardoso JV, Reimer J, Harrington J, Rodríguez JLC, Nunez-Iglesias J, Kuczynski J, Tritz K, Thoma M, Newville M, Kümmerer M, Bolingbroke M, Tartre M, Pak M, Smith NJ, Nowaczyk N, Shebanov N, Pavlyk O, Brodtkorb PA, Lee P, McGibbon RT, Feldbauer R, Lewis S, Tygier S, Sievert S, Vigna S, Peterson S, More S, Pudlik T, Oshima T, Pingel TJ, Robitaille TP, Spura T, Jones TR, Cera T, Leslie T, Zito T, Krauss T, Upadhyay U, Halchenko YO, and YV-B, SciPy 1.0: fundamental algorithms for scientific computing in Python, Nature Methods 17 (3) (2020) 261–272, 10.1038/s41592-019-0686-2. [PubMed: 32015543]

[20]. Galende E, Karakikes I, Edelmann L, Desnick RJ, Kerenyi T, Khoueiry G, Lafferty J, McGinn JT, Brodman M, Fuster V, Hajjar RJ, Polgar K, Amniotic fluid cells are more efficiently reprogrammed to pluripotency than adult cells, Cell. Reprogr. 12 (2) (2010) 117–125, 10.1089/cell.2009.0077, Publisher: Mary Ann Liebert, Inc..

[21]. Serrao GW, Turnbull IC, Ancukiewicz D, Kim DE, Kao E, Cashman TJ, Hadri L, Hajjar RJ, Costa KD, Myocyte-depleted engineered cardiac tissues support therapeutic potential of mesenchymal stem cells, Tissue Eng. A 18 (13–14) (2012) 1322–1333, 10.1089/ten.tea.2011.0278, Publisher: Mary Ann Liebert Inc..

[22]. Rupert CE, Kim TY, Choi BR, Coulombe KL, Human cardiac fibroblast number and activation state modulate electromechanical function of hiPSC-cardiomyocytes in engineered myocardium, Stem Cells Int. 2020 (2020) 10.1155/2020/9363809, Publisher: Hindawi Limited.

[23]. R Core Team R: A Language and Environment for Statistical Computing, R Foundation for Statistical Computing, 2021, URL https://cran.r-project.org.

[24]. Dostanić M, Windt LM, Stein JM, van Meer BJ, Bellin M, Orlova V, Mastrangeli M, Mummery CL, Sarro PM, A miniaturized EHT platform for accurate measurements of tissue contractile properties, J. Microelectromech. Syst. 29 (5) (2020) 881–887, 10.1109/JMEMS.2020.3011196.

[25]. Hinson JT, Chopra A, Nafissi N, Polacheck WJ, Benson CC, Swist S, Gorham J, Yang L, Schafer S, Sheng CC, Haghighi A, Homsy J, Hubner N, Church G, Cook SA, Linke WA, Chen CS, Seidman JG, Seidman CE, Titin mutations in iPS cells define sarcomere insufficiency as a cause of dilated cardiomyopathy, Science 349 (6251) (2015) 982–986, 10.1126/science.aaa5458. [PubMed: 26315439]

[26]. Tandon N, Cannizzaro C, Chao PHG, Maidhof R, Marsano A, Au HTH, Radisic M, Vunjak-Novakovic G, Electrical stimulation systems for cardiac tissue engineering, Nat. Protoc. 4 (2) (2009) 155–173, 10.1038/nprot.2008.183, Publisher: Nature Publishing Group. [PubMed: 19180087]

[27]. Goldfracht I, Protze S, Shiti A, Setter N, Gruber A, Shaheen N, Nartiss Y, Keller G, Gepstein L, Generating ring-shaped engineered heart tissues from ventricular and atrial human pluripotent stem cell-derived cardiomyocytes, Nature Commun. 11 (1) (2020) 75, 10.1038/s41467-019-13868-x. [PubMed: 31911598]

[28]. Kerscher P, Turnbull IC, Hodge AJ, Kim J, Seliktar D, Easley CJ, Costa KD, Lipke EA, Direct hydrogel encapsulation of pluripotent stem cells enables ontomimetic differentiation and growth of engineered human heart tissues, Biomaterials 83 (2016) 383–395, 10.1016/j.biomaterials.2015.12.011, Publisher: Elsevier. [PubMed: 26826618]

[29]. Nakane T, Masumoto H, Tinney JP, Yuan F, Kowalski WJ, Ye F, Leblanc AJ, Sakata R, Yamashita JK, Keller BB, Impact of cell composition and geometry on human induced pluripotent stem cells-derived engineered cardiac tissue, Sci. Rep. 7 (1) (2017) 1–13, 10.1038/srep45641, Publisher: Nature Publishing Group. [PubMed: 28127051]

[30]. Hansen A, Eder A, Bönstrup M, Flato M, Mewe M, Schaaf S, Aksehirlioglu B, Schwörer A, Uebeler J, Eschenhagen T, Development of a drug screening platform based on engineered heart tissue, Circ. Res. 107 (1) (2010) 35–44, 10.1161/CIRCRESAHA.109.211458, Publisher: Lippincott Williams & Wilkins. URL [PubMed: 20448218]

[31]. Tiburcy M, Hudson JE, Balfanz P, Schlick S, Meyer T, Liao M-LC, Levent E, Raad F, Zeidler S, Wingender E, Riegler J, Wang M, Gold JD, Kehat I, Wettwer E, Ravens U, Dierickx P, van Laake LW, Goumans MJ, Khadjeh S, Toischer K, Hasenfuss G, Couture LA, Unger A, Linke WA, Araki T, Neel B, Keller G, Gepstein L, Wu JC, Zimmermann W-H, Defined engineered human myocardium with advanced maturation for applications in heart failure modeling and repair, Circulation 135 (19) (2017) 1832–1847, 10.1161/circulationaha.116.024145. [PubMed: 28167635]

[32]. Murphy JF, Mayourian J, Stillitano F, Munawar S, Broughton KM, Agullo-Pascual E, Sussman MA, Hajjar RJ, Costa KD, Turnbull IC, Adult human cardiac stem cell supplementation effectively increases contractile function and maturation in human engineered cardiac tissues, Stem Cell Res. Ther. 10 (1) (2019) 10.1186/s13287-019-1486-4, Publisher: Springer Science and Business Media LLC.

[33]. Mayourian J, Ceholski D, Gorski P, Mathiyalagan P, Murphy J, Salazar S, Stillitano F, Hare J, Sahoo S, Hajjar R, Costa K, Exosomal microRNA-21–5p mediates mesenchymal stem cell paracrine effects on human cardiac tissue contractility, Circ. Res. 122 (7) (2018) 933–944, 10.1161/CIRCRESAHA.118.312420. [PubMed: 29449318]

[34]. Held D, Thrun S, Savarese S, Learning to track at 100 FPS with deep regression networks, in: European Conference Computer Vision (ECCV), 2016, URL https://arxiv.org/abs/1604.01802v2.

[35]. Rosebrock A, OpenCV shape detection, 2021, URL https://www.pyimagesearch.com/2016/02/08/opencv-shape-detection/.

[36]. Pathak AR, Pandey M, Rautaray S, Application of deep learning for object detection, Procedia Comput. Sci. 132 (2018) 1706–1717, 10.1016/j.procs.2018.05.144, Publisher: Elsevier.

[37]. Teles D, Kim Y, Ronaldson-Bouchard K, Vunjak-Novakovic G, Machine learning techniques to classify healthy and diseased cardiomyocytes by contractility profile, ACS Biomater. Sci. Eng. 7 (2021) 3043–3052, 10.1021/acsbiomaterials.1c00418, Publisher: American Chemical Society. [PubMed: 34152732]

[38]. Han JJ, FDA Modernization Act 2.0 allows for alternatives to animal testing, Artif. Organs (2023) 10.1111/aor.14503.

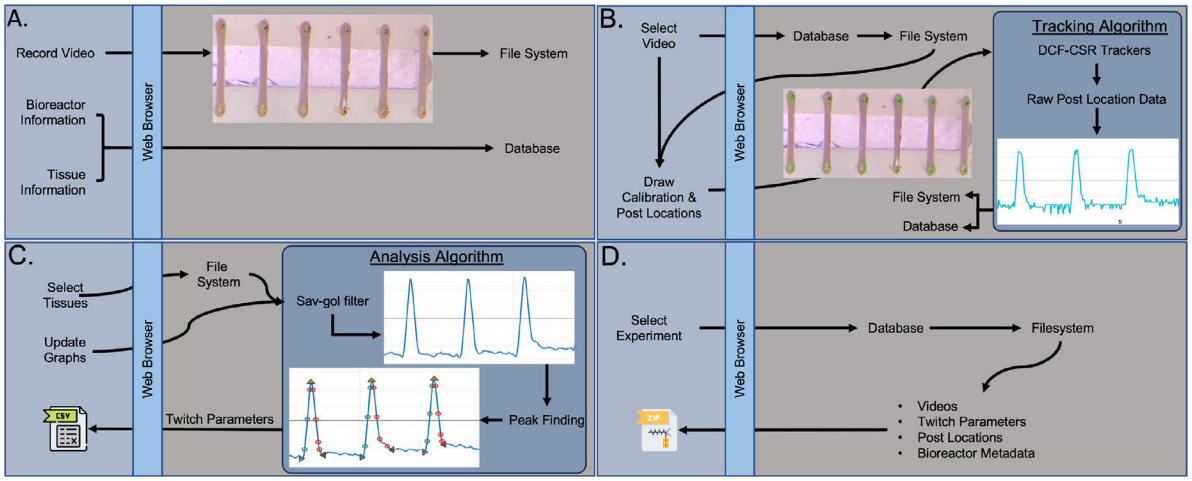

Fig. 1.

Rianú workflow overview. (A) Uploading workflow. Recorded videos are saved to the server's file system, while bioreactor and tissue metadata is stored in the database. The inset photograph is a top view of an array of six hECTs suspended between cantilever posts. (B) Tracking workflow. A video is selected from the uploaded videos by the user and collected by Rianú, the user draws post location on the first frame (green boxes on inset photograph), the tracking algorithm tracks posts and saves displacements. (C) Analysis workflow. Tissues of interest that have been tracked are selected by the user. Rianú filters the data, finds peaks, and calculates twitch parameters. The analysis algorithm can be recalled to update graphs with new sav-gol filter parameters, new peak finding parameters, or a reduced time interval of interest for each tissue. (D) Archiving workflow. An experiment is selected by the user. Rianú finds all videos associated with that experiment and saves those videos along with the calculated twitch parameters, post locations, and bioreactor metadata in a zip file. This zip can be later uploaded for further analysis as needed. The web browser (sky blue) represents the interface between the user inputs and outputs (blue-gray; left) and the server actions (gray; right).

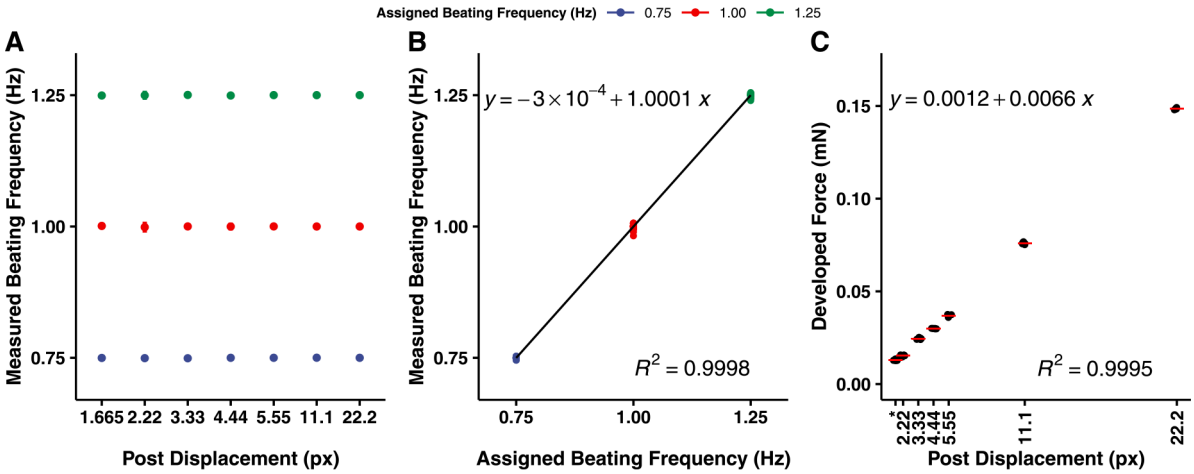

Fig. 2.

In-silico characterization of Rianú. (A) The measured beating frequency after tracking simulated hECTs at varying assigned frequencies (blue: 0.75; red: 1.00; green: 1.25 Hz) and post displacement amplitudes. Values shown represent mean and error bars represent standard deviation. (B) Linear least-squares regression model comparing measured beating frequency and assigned beating frequency. Values shown represent individual simulated tissues. (C) Linear least-squares regression model showing the calculated developed force at different post deflections at 1.00 Hz. * is 1.665 post displacement (px). Values shown represent individual simulated tissues, crossbar (red line) represents the mean. n = 6 simulated tissues per post displacement group at each frequency (total n = 126; panels A and B), n = 6 simulated tissues per post displacement (total n = 42; panel C).

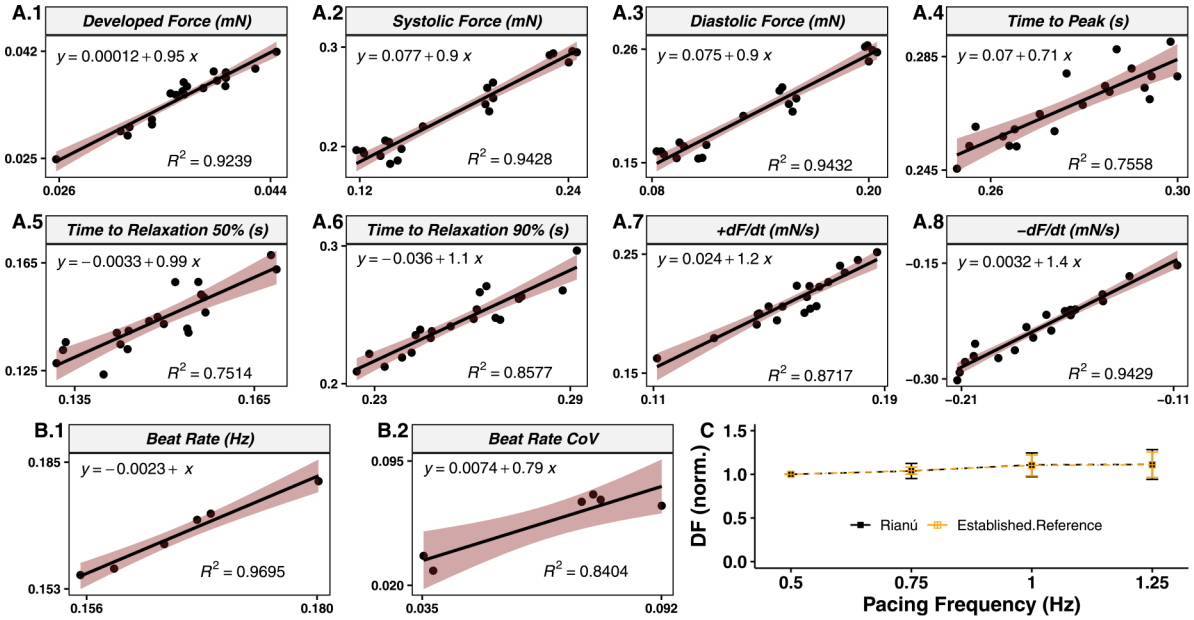

Fig. 3.

Comparison of Rianú with our established reference software. Twitch characteristics of electrically stimulated (A, n = 7 at 0.75 Hz, n = 7 at 1.00 Hz, and n = 6 at 1.25 Hz) and spontaneously beating (B, n = 6) twitch characteristics of hECTs calculated independently by the current established reference (x-axis) and Rianú (y-axis). Solid black lines represent results of linear regression (best-fit equation shown) and red shaded regions represent 95% confidence intervals. Force-frequency relationship (C) of electrically stimulated tissues normalized to 0.5 Hz for each hECT, with mean ± standard deviation for Rianú (solid black square, dashed black line) and current established reference (hollow orange box with crosshair, dashed orange line), DF = Developed force.

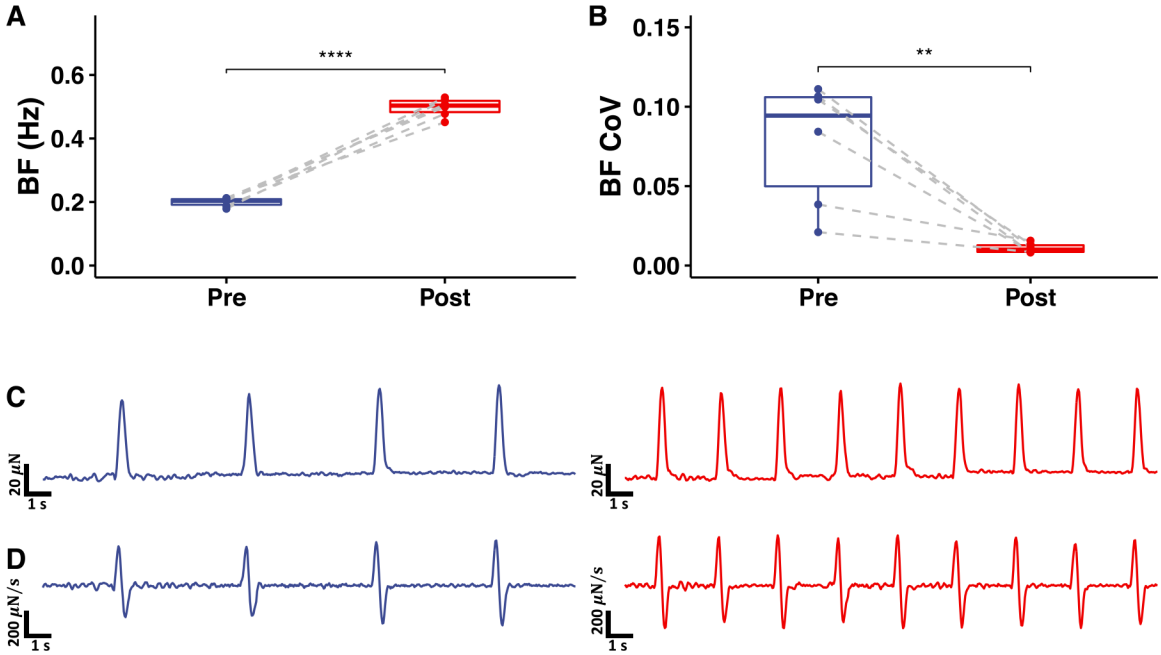

Fig. 4.

Isoproterenol induced chronotropic effects on hECT. (A) Spontaneous beating frequency, (B) spontaneous beating frequency coefficient of variation, (C) representative twitch force tracings, and (D) representative dF/dt tracings of hECT before (blue) and ten minutes after (red) isoproterenol treatment [300 nM] are displayed. n = 6 hECT. Boxplots represent minimum, Q1, median, Q3, maximum. ** $P < 0.01$, and **** $P < 0.0001$.

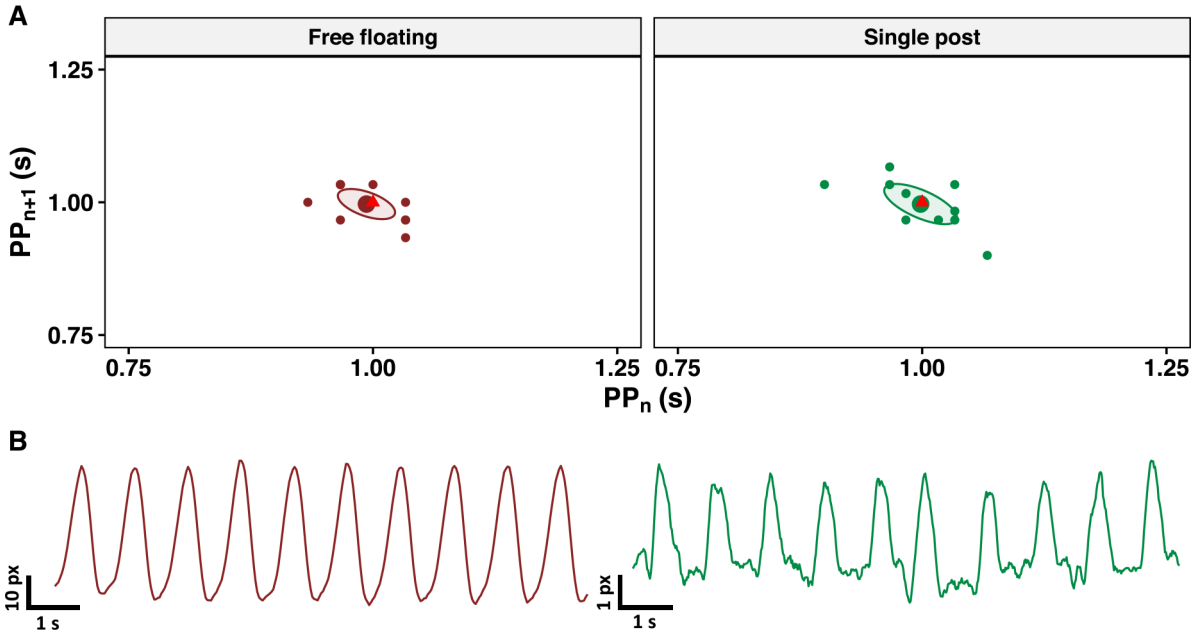

Fig. 5.

Non-cantilever applications. (A) Poincaré plot of time to next peak (PP_{n+1}) and time to previous peak (PP_n) with the supplied electrical field stimulation (red triangle) indicated. Ellipse represents 95% confidence interval of the mean. PP = peak-to-peak. (B) Ten second twitch tracings from free-floating (brown) and single post anchored (green) tissues. Note different scale for *y* axes.

Table 1.

List of cardiac muscle function parameters analyzed by Rianú.

Parameter	Abbrev.	Definition
Developed force (mN)	DF	Difference between peak (systolic) and baseline (diastolic) force.
Time to peak force (s)	T2PK	Time to reach peak force from 10% contracted.
Time to 50% relaxation (s)	R50	Time between peak force and 50% of the relaxation.
Time to 90% relaxation (s)	R90	Time between peak force and 90% of the relaxation.
Maximum rate of contraction (mN/s)	+dF/dt	Maximum of the first-order derivative of the force tracing with relation to time.
Maximum rate of relaxation (mN/s)	−dF/dt	Minimum of the first-order derivative of the force tracing with relation to time.
Beating frequency (Hz)	BF	Peak-to-peak interval^{-1}
BF coefficient of variation	BF CoV	Standard deviation of the beating frequency divided by the beating frequency

Comput Methods Programs Biomed Update. Author manuscript; available in PMC 2023 July 20.